water

MDPI

Article

Use of Sawdust (*Aspidosperma polyneuron*) in the Preparation of a Biocarbon-Type Adsorbent Material for Its Potential Use in the Elimination of Cationic Contaminants in Wastewater

Rodrigo Ortega-Toro [1,*], Ángel Villabona-Ortíz [2], Candelaria Tejada-Tovar [2], Adriana Herrera-Barros [3] and Daniela Cabrales-Sanjuan [2]

[1] Food Packaging and Shelf-Life Research Group (FP&SL), Food Engineering Department, Universidad de Cartagena, Avenida del Consulado St. 30, Cartagena de Indias 130015, Colombia
[2] Process Design and Biomass Utilization Research Group (IDAB), Chemical Engineering Department, Universidad de Cartagena, Avenida del Consulado St. 30, Cartagena de Indias 130015, Colombia; avillabonao@unicartagena.edu.co (Á.V.-O.); ctejadat@unicartagena.edu.co (C.T.-T.); cabralesdaniela97@gmail.com (D.C.-S.)
[3] Research Group, Nanomaterials and Computer-Aided Process Engineering (NIPAC), Chemical Engineering Department, Universidad de Cartagena, Avenida del Consulado St. 30, Cartagena de Indias 130015, Colombia; aherrerab2@unicartagena.edu.co
* Correspondence: rortegap1@unicartagena.edu.co

Abstract: Chemically modified bioadsorbents were prepared using sawdust (Aspidosperma polyneuron) functionalized with urea at different concentrations (BC-1M, BC-3M, and BC-6M) to evaluate their adsorption capacity by the methylene blue method. Fourier transform spectroscopy (FTIR) analysis and scanning electron microscopy (SEM) were employed to characterize the surface morphology of the biomaterials. The best adsorption capacity was obtained using the biocarbon modified with urea 6M (BC-6M), displaying a methylene blue index of 12.4 mg/g with a zero-charge point (pHpzc) at 5.5, suggesting the potential application of this chemically modified bioadsorbent for the removal of cationic contaminants in aqueous media.

Keywords: methylene blue; Sawdust; carbon-like biomaterial; adsorption capacity

Citation: Ortega-Toro, R.; Villabona-Ortíz, Á.; Tejada-Tovar, C.; Herrera-Barros, A.; Cabrales-Sanjuan, D. Use of Sawdust (*Aspidosperma polyneuron*) in the Preparation of a Biocarbon-Type Adsorbent Material for Its Potential Use in the Elimination of Cationic Contaminants in Wastewater. *Water* **2023**, *15*, 3868. https://doi.org/10.3390/w15213868

Academic Editor: John Zhou

Received: 28 July 2023
Revised: 12 September 2023
Accepted: 15 September 2023
Published: 6 November 2023

1. Introduction

The textile industry promotes economic development. It generates many jobs, encourages the cultivation of natural fiber sources, and harnesses resources from the petrochemical industry, such as synthetic fibers, to produce various textiles [1]. However, this industry generates many negative environmental impacts, including indiscriminate water use. The textile industry is estimated to use more than 11,000 L of water for every kilogram of natural fiber processed [2]. These waters have high concentrations of pollutants, including various dyes. In this sense, the discharge of colored wastewater without prior treatment is of concern since the concentrations of synthetic dyes in the body can cause multiple pathologies in humans and animals because they are genotoxic, mutagenic, and carcinogenic [3]. In flora, the damage is evident in the reduction in germination and growth of some plants. Therefore, eliminating dyes in water from the textile industry is essential [4].

Treatment methods for colored water include electrocoagulation, flocculation, reverse osmosis, and adsorption, among others [5]. Adsorption has the advantage of being one of the cheapest technologies; however, commercial adsorbents are expensive to produce. Consequently, recent research studies have focused on evaluating other adsorbents made from various natural and synthetic materials. The possibility of using waste biomasses to prepare adsorbents has attained the scientific community's attention because of their availability and low cost [6,7]. Previous studies have registered the use of various waste biomasses for the preparation of bioadsorbents, such as orange peel [8], pineapple peel [9], mixed sawdust [7],

and corn stover [10], among others. Furthermore, Alshammari and coworkers [11] reported the preparation of a bioadsorbent using shrimp shells as a waste biomaterial. In that work, they evaluated the synthesis of substituted polyaniline-based nanoparticles with chitosan grafts from shrimp shells as a promising biomaterial for dye removal [11].

It has been reported that the wastes from the wood industry have the potential to be used as adsorbent materials. Bortoluz et al. [12] conducted a study to evaluate the potential of Pinus elliottii sawdust as a bioadsorbent for removing methylene blue (MB) dye in aqueous media. In this work, the sawdust was subjected to a sequential extraction process using different solvents to improve its adsorption properties. Various techniques were used to characterize the sawdust, including morphological and spectroscopic analyses. Moreover, it was analyzed the impact of experimental variables on the adsorption process, including contact time (2–240 min), pH (3.0–10.0), stirring speed (90–210 rpm), adsorbent dose (1.0–5.0 g/L), and initial MB concentration (60–140 mg/L). In addition, the equilibrium, kinetic, and thermodynamic analyses were performed, and it was found that the MB removal rate was approximately 97%, mainly due to physisorption. The Freundlich model best described the experimental data, while the kinetic data best fit the pseudo-second-order model. These results suggest that this adsorbent can effectively remove cationic dyes from textile wastewater.

In a study performed by Bhowmik et al. [13], raw sawdust was utilized to prepare two chemically activated carbons. One was treated with orthophosphoric acid, and the other with sodium hydroxide. Both activated carbons were obtained in a furnace at a temperature of 973 K and tested in batch mode to determine their efficacy in removing indigo carmine dye. The thermodynamic results indicated that the process was exothermic, and the activated carbon produced after activation with orthophosphoric acid proved to have a superior removal capacity and efficiency. Moreover, its adsorption capacity reached 9.39 mg/g, compared to 6.74 mg/g for hydroxide-activated carbon. This study shows that inexpensive waste materials, such as sawdust, can efficiently remove anionic dyes.

On the other hand, the research carried out by Sun et al. [14] consisted of the elaboration of a biochar from eucalyptus sawdust modified with citric, tartaric, and acetic acid at low temperatures to eliminate the blue of methylene (MB) from aqueous solutions. The material was characterized by FTIR. Furthermore, the adsorption process was evaluated by applying Langmuir, Freundlich, Temkin isotherms, pseudo-first and second-order kinetic models, intraparticle diffusion, Elovich, and Weber–Morris models. The maximum adsorption capacities of the biochars modified with the citric, tartaric, and acetic acids were 178.57, 99.01, and 29.94 mg/g, respectively, at 35 °C. Additionally, Oyewo et al. [15] reported the preparation and application of sawdust-derived cellulose mono-crystals with zinc oxide nanoparticles (CNC/ZnO) as a new adsorbent material for removing methylene blue in solution. The adsorbent material was characterized by FTIR analysis, X-ray diffraction (XRD), and scanning electron microscopy (SEM). In this study, it was shown that impregnation with ZnO nanoparticles improved the crystallinity of the adsorbent. The results showed that the CNC/ZnO presented good performance in the adsorption of methylene blue, achieving a maximum adsorption capacity of 64.93 mg/g, adjusting to the Langmuir isotherm and the pseudo-second-order kinetic model.

Consequently, the focus of this research project is on creating carbon-based biomaterials utilizing sawdust from *Aspidosperma polyneuron* (AAP), harvested from sawmills in Cartagena, Colombia. The goal is to explore the potential of these biomaterials for adsorption using the methylene blue method. The bio adsorbents are analyzed using Fourier transform spectroscopy (FTIR) both before and after the adsorption process. The results of this study contribute towards sustainable technological development by describing the characteristics of a potential adsorbent. Improving these data can aid in selecting an efficient and cost-effective adsorbent for the removal of textile dyes, leading to reduced costs in wastewater treatment processes, control of water body pollution, and the utilization of sawdust of *Aspidosperma polyneuron* (AAP) for an alternative purpose. Furthermore, this research expands the available literature on the evaluation of chemically modified coals made from sawdust, addressing the current need for more information on this topic.

2. Materials and Methods

In the following, the methodology carried out for the preparation of the biomaterials, characterization techniques, and the determination of the methylene blue adsorption rate will be described.

2.1. Aspidosperma Polyneuron Sawdust Pre-Treatment

The sawdust was washed at room temperature with 80 °C deionized water to remove impurities and unwanted substances. Subsequently, it was dried in the sun for 6 h and in an oven at 70 °C for 8 h. The dry sawdust was introduced into a muffle with a heating rate of 5 °C/min up to 250 °C. The equipment is turned off at the end of the process, and the muffle is left to rest and preserved. An evaluation of the carbonization temperature and the residence time of the biomass in the muffle was carried out to determine the values of these variables to carry out the carbonization [16].

Afterward, a portion of the biochar was taken, washed, and dried in an oven at 100 °C for 2 h. Then, the bioadsorbent was packaged and labeled as unmodified biochar (CCS) to be used as a control. The remaining portion was mixed with distilled water in a 1:3 ratio, shaken, and placed in an ultrasonic bath for one minute; then, this material was vacuum filtered and dried for two hours in an oven at 100 °C. Subsequently, the dried biomaterial is mixed in a beaker with a 50% phosphoric acid solution, with a ratio of 1 g per each 5 mL of solution, using constant stirring at 100 °C for 3 h [16]. Afterward, this biomaterial was washed, vacuum filtered, and dried to perform urea functionalization. For this chemical modification, the biomaterials were mixed with urea solutions at three different concentrations: 1 M, 3 M, and 6 M in a ratio of 1 g:5 mL, placed in a shaker for 18 h, then vacuum filtered and dried in an oven at 100 °C, as shown in Figure 1. Adding urea to sawdust during the functionalization process significantly impacts its ability to adsorb contaminants [17]. This is because urea chemically interacts with the surface of the sawdust particles, modifying their characteristics, such as their charge and affinity for specific pollutants [18]. The concentration of urea used can also affect the structure and porosity of the material, which directly affects its ability to interact with contaminants in a solution [19]. By incorporating urea, the adsorption capacity can be increased, and the selectivity of the adsorbent towards specific pollutants can be improved [18].

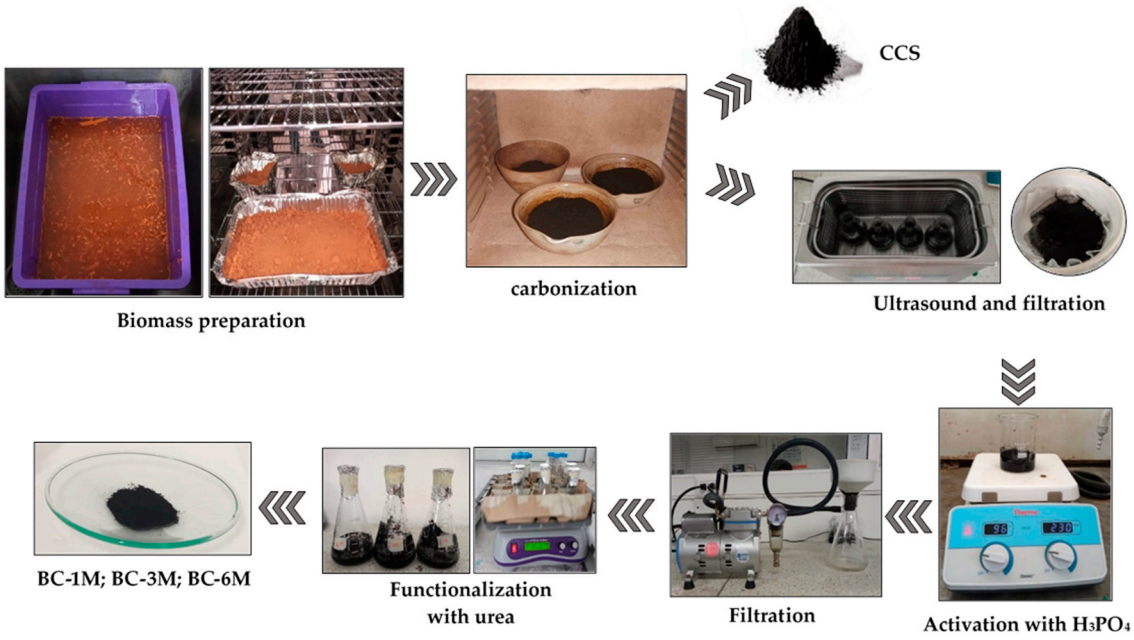

Figure 1. Preparation of urea-modified carbon-type biomaterials.

2.2. Characterization of Biomaterial-Type Carbon

To characterize the AAP and biomaterial, particle size analysis was carried out, following the ASTM standard [20]; for this, a shaker-type sieve shaker with seven sieves with mesh numbers (2, 1, 0.5, 0.355, 0.212, 0.15, and 0.106 mm) was used. The variation in the percentage of particle sizes in the sawdust was determined. The adsorbents were characterized by FTIR analysis before and after the methylene blue adsorption process to identify the main functional groups in the modified and unmodified biomasses.

A test tube was used to calculate apparent density, into which a specific amount of solid with a known mass was introduced, and the ratio of mass to volume was calculated [21]. For the calculation of the real density, an empty pycnometer was initially weighed and filled with water up to the mark; then, the pycnometer was weighed with a sample of solid inside, and water was added up to the mark to the pycnometer with the sample and weighed; the real density was calculated considering Equation (1).

$$\rho_{real} = \frac{m_A\, \rho_L}{m_A + m_L - m_{A,L}} \quad (1)$$

where m_A is the mass of adsorbent in g, ρ_L is the density of the liquid in g/cm^3, m_L is the mass of the liquid in g, and $m_{A,L}$ is the mass of the adsorbent with liquid in g.

The porosity of the sawdust and the biomaterials were calculated considering Equation (2) and the determined values of apparent density and real density of the samples.

$$(\%)\varphi = \frac{\rho_r - \rho_a}{\rho_r} \times 100 \quad (2)$$

where ρ_r and ρ_a are the real and apparent densities, g/cm^3, respectively.

For the determination of the pH at the zero-charge point (pHpzc) of the biomaterial, 0.05 g of each biomaterial was placed in contact with 5 mL of distilled water in test tubes; the pH was adjusted between 3 and 11, using 0.1 N sodium hydroxide and 0.1 N hydrochloric acid solutions. The mixture was kept for 24 h in a shaker at 200 rpm and room temperature. Finally, the pH was measured after this time, and the pH difference was compared graphically [22].

2.3. Adsorption Tests

Adsorption tests were performed according to ASTM [23]. For this purpose, an adsorption test was performed with a single dependent variable: the pH of the initial solution, using the cationic dye Methylene Blue (MB) as a contaminant. The incidence of the initial pH of the solution was evaluated by defining 3 pH levels above pHpzc, keeping the adsorbent dose (0.035 g), the contaminant concentration (40 mg/L), and the volume of the solution (10 mL) constant at room temperature, with agitation at 200 rpm for 24 h. The above considers the cationic nature of the pollutant and the need to deprotonate the adsorbent surface to encourage the attractive forces between methylene blue and the synthesized biomaterials [24]. All experiments were performed in duplicate.

The adsorption capacity of each biomaterial was determined by centrifuging test tubes at 5000 rpm for 5 min. The absorbance of MB was then measured at 664 nm using a Biobase model BK-UV1900 UV-VIS spectrophotometer, acquired from the manufacturer Biobase Group, Jinan, Shandong, China. Next, the adsorption of methylene blue was evaluated under the best pH condition previously identified. At room temperature, the adsorbent dose and the contaminant concentration were kept constant at 0.035 g and 60 mg/L, respectively. Each experiment was replicated by adding 10 mL of solution to each test tube and shaking it for 24 h on a shaker.

The removal efficiency (R_E) was determined using Equation (3) [25].

$$(\%)R_E = \left[\frac{C_O - C_T}{C_O} \times 100\right] \quad (3)$$

where C_O and C_T are the initial and final dye concentrations in an aqueous solution.

The results were processed with Statgraphics Centurion XVI software to determine the significant variables of the process through an analysis of variance ANOVA, which is used to evaluate a null hypothesis (H_0), suggesting that the solution's initial pH does not significantly affect the methylene blue index, and an alternative theory (H_a), which postulates that the initial pH of the solution does influence the methylene blue index [26].

The adsorption capacity was determined using Equation (4).

$$q_e = \frac{(C_O - C_T) \times V}{m} \quad (4)$$

where q_e is the concentration of methylene blue in the adsorbent (mg/g); C_O and C_T are the initial and final concentration of dye in aqueous solution (mg/L); V is the volume of solution (L), and m is the mass of adsorbent (g) [27].

3. Results

The results of the work are presented and discussed below.

3.1. Biomaterial Synthesis

According to Sajjadi et al. [16], a temperature of 500 °C and a residence time in the oven of 3 h were examined for carbonization. However, low yield of char formation and the presence of ash were detected. Therefore, a review of these two variables listed in Table 1 was conducted.

Table 1. Effect of varying carbonization temperature and residence time on the percentage yield of char.

Carbonization Temperature (°C)	Dwell Time (h)	Initial Mass (g)	Final Mass (g)	Yield (%)	Ash in the Final Mass
500	3	50	0.8	1.6	Yes
500	2	50	0.8	1.6	Yes
250	1	50	4.2	8.4	No
250	$\frac{1}{2}$	50	6.3	12.6	No

The best carbon formation results were observed at the lowest temperature and residence time conditions, 250 °C and 30 min, respectively. The presence of ash in the final carbon-rich mass can be attributed to the oxygen present during the carbonization process [28]. It is crucial to minimize the percentage of oxygen during the carbonization process to improve the performance of the bioadsorbent, similar to a pyrolytic process [29,30]. However, considering scenarios where a pyrolytic furnace is inaccessible, alternative methods are possible, such as obtaining muffle coals with favorable characteristics. For example, Nath et al. [31] synthesized charcoal from sawdust mixtures, producing a methylene blue index of 78.1 mg/g, with carbonization temperatures of 400 °C. This evaluation highlights how carbonization variables and raw material characteristics, such as moisture content and porosity, influence biomaterials' properties, as suggested by Prías et al. [32].

3.2. Characterization of Bioadsorbents

Table 2 shows the results of the calculation of the apparent density of AAP and the coals synthesized from it (Table A1 presents the calculated values in Appendix A). The samples displayed similar bulk densities, with the highest value being observed for AAP. However, it is important to note that porosity does not necessarily follow the trend of increased bulk density after carbonization. In the case of biomaterials made from sawdust, the difference in particle size between the initial sawdust and the resulting biomaterial is responsible for the differences in bulk density. The initial sawdust has a larger particle size, influenced by different structural components such as lignin, cellulose, and hemicellulose that get released during carbonization [33].

Table 2. Density and porosity values of the biosorbents prepared from *Aspidosperma polyneuron* (AAP) sawdust, unmodified biochar (CCS), and modified biochars (BC-1M, BC-3M, and BC-6M).

Sample	Volume (cm^3)	Apparent Density (g/cm^3)	Real Density (kg/cm^3)	Porosity %
AAP	3	0.360	2.455	85.3
CCS	3	0.280	0.296	0.5
BC-1M	3	0.310	0.327	5.1
BC-3M	3	0.303	0.308	1.8
BC-6M	3	0.310	0.783	60.4

Additionally, as expected, a difference was observed between the real and apparent densities in each biomaterial. However, the difference between the real and apparent density of the biomaterial is low, except for BC-6M; this can be attributed to the fact that the sample BC-6M was functionalized with the highest urea concentration, which increased the mass of biomaterial as compared with the samples BC-1M and BC-3M. Phosphoric acid activation increased porosity by 59.9% in modified biochars (detailed values are shown in Table A2 of Appendix A). The porosity of BC-6M sample is higher than that found for various coals, such as the coal synthesized from Marabu, reported by Prieto et al. [34], carbonized at 400 °C for 1 h, obtaining a porosity of 52.5%.

The size distribution of coals depends on the composition of the biomass used as raw material and the carbonization process, as mentioned by Velázquez-Maldonado et al. [35], hence the importance of analyzing the characteristics of AAP. Table 3 presents the size distribution results, showing that 6.1% of the AAP sample has a mean particle size of 1.5 mm, 32.1% a particle size of 0.75 mm, 13. 6% have a particle size of 0.428 mm, 20% a particle size of 0.284 mm, 10.8% a particle size of 0.181 mm, 9.5% a particle size of 0.128 mm, and the remaining 8.5% have a particle size smaller than 0.106 mm.

Table 3. Estimation of fraction retained and cumulative retained from sieve data.

Mass (g)		Mesh	Aperture (mm)	D_{pi} (mm)	(ΔØ)	(ØR)
-	-	10	2	-	-	-
m1	10.7	18	1	1.5	0.061	0.061
m2	56.4	35	0.5	0.75	0.321	0.382
m3	23.8	45	0.355	0.428	0.136	0.518
m4	35.1	70	0.212	0.284	0.200	0.718
m5	19.0	100	0.15	0.181	0.108	0.826
m6	16.6	140	0.106	0.128	0.095	0.920
m7	14	Bottom	Bottom	-	0.080	1.000
M_T	175.6	-	-	-	1	-

Note(s): where D_{pi}: mean particle diameter. ΔØ: retained fraction. ØR: cumulative retained fraction.

Approximately 48% of the sawdust fraction has a particle size smaller than 0.428 mm, which implies that the biomaterial will have a higher percentage of this particle size, obtaining a char with finer particles than other previously studied charcoals, such as rice husk charcoal, carbonized at 200 °C by hydrothermal carbonization, where a 55.26% by weight of the total sample, for particle sizes between 0.86 and 2.38 mm [35]. The high percentage of fine particles can favor the adsorption of the textile dyes to be evaluated due to the increased surface area values expected for this type of biomaterial. It has also been identified that fine biomaterial can perform well when used as aggregates for productive soils because it is easier to mix with the soil, allowing the formation of a homogeneous mixture of both components [36].

The design processes of silos in solids handling for the storage of adsorbents used for adsorption at the industrial level require data on size distribution analysis by sieving; therefore, the data presented from the study of sawdust are essential for a possible subsequent industrial implementation in addition to indicating an estimate of the size distribution of

biomaterial which shows particle size values lower than those found for sawdust due to the decrease in particle size of the biomass in the carbonization process [37].

When analyzing the sawdust particles of *Aspidosperma polyneuron* (AAP), the density of 2455 kg/cm^3 was taken into consideration to determine the surface-volume diameter, mass mean diameter, and arithmetic mean diameter (values are shown in Table A3 in Appendix A). The diameter data obtained indicated that the AAP sawdust has a small particle size compared to other woods, such as carob, majagua, and cedar, which exhibit larger particle sizes of 1.59, 3.2, and 4.8 mm, respectively [38]. The average mass diameter of the AAP sawdust is 0.479 mm, which is advantageous for adsorption as the charcoal synthesized from AAP has a particle size smaller than 0.428 mm, leading to a high surface area [38,39].

3.3. Zero Loading Point pH$_{pzc}$

Low pH$_{pzc}$ values of 3.35, 3.6, and 5.6 were found for the biomaterials functionalized with urea BC-1M, BC-3M, and BC-6M. This indicates that these biomaterials favor the adsorption of cationic contaminants in solutions with a pH higher than the pH$_{pzc}$ found for each biomaterial. In comparison, the adsorption of anionic contaminants is favored in solutions with lower pH (see Figure 2). In the case of unmodified charcoal (CCS) and sawdust from *Aspidosperma polyneuron* (AAP), a pH$_{pzc}$ of 5.6 and 8.1, respectively, was found. These data were evaluated to obtain comparison values and provide information for future experiments where CCS and AAP are considered adsorbents.

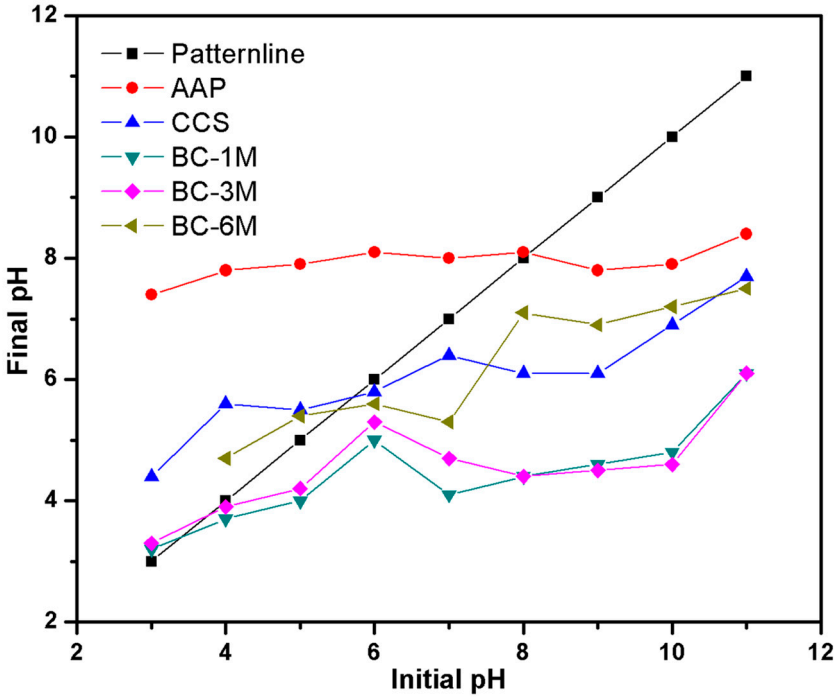

Figure 2. Evaluation of the pH$_{pzc}$ of AAP, CCS, BC-1M, BC-3M, and BC-6M.

A pH$_{pzc}$ for the AAP of 8.1 is observed, indicating alkalinity, while the value for CCS presented a value indicating acidity (5.6). The latter result agrees with those found by Prieto et al. [40], who synthesized biomaterial from red variety sugarcane bagasse, obtaining a value of 6.1, which was then heated at 800 °C for 120 min and chemically modified only with phosphoric acid at 0.6 mol/L: the residence time and carbonization temperature allow the release of a higher concentration of substances that contribute to the acidity of the adsorbent, which is why the pH$_{pzc}$ values differ. For their part, Daza et al. [41] evaluated the pH$_{pzc}$ of a biomaterial physically activated with steam made from bituminous mineral coal, obtaining a value of 5.6 in both cases.

On the other hand, a decrease in the pH_{pzc} of the functionalized biomaterial concerning the unmodified CCS coal is observed, indicating an increase in its acidity. This behavior is related to the acidic nature of the modifying agents, which affects the final pH of the adsorbent; a similar behavior is observed in the pH_{pzc} of biomaterial synthesized from a mixture of sawdust by Nath et al. [31], obtained a value of 4.8 for this biomaterial, while the biomaterial modified with NaOH and coated with a biopolymer made from okra mucilage presented a value of 7.95; an increase in alkalinity related to the modifying agents is observed. In the case of the biomaterials modified in this study, it is assumed that to favor the adsorption of cationic pollutants, the pH of the solution must be adjusted above the pH_{pzc} value found for each one, because in solutions with pH higher than pH_{pzc} there is a more significant presence of negatively charged ions, favoring the adsorption of cations.

3.4. FTIR Analysis

FTIR spectra were compared to determine the difference in the functional groups of the biomass, sawdust, and unmodified biomaterial. Figure 3 shows the differences between the infrared spectra of the bio adsorbents under study.

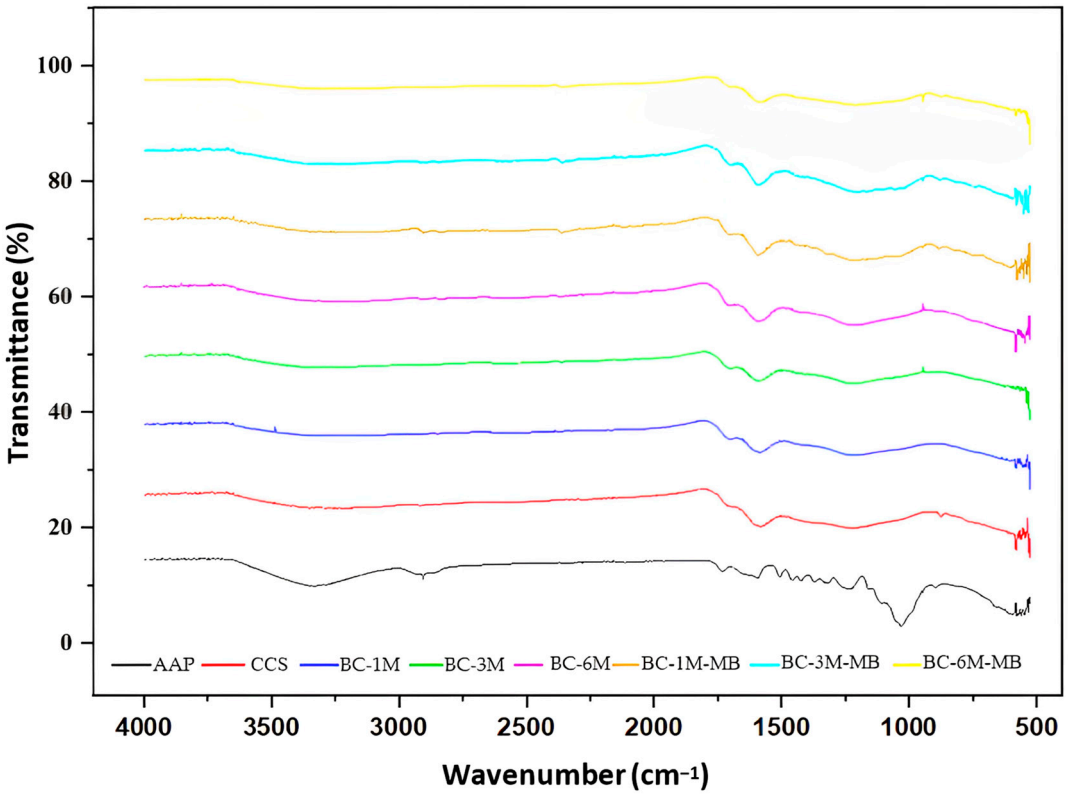

Figure 3. FTIR analysis of the adsorbents evaluated with the methylene blue test (after and before the adsorption process) (BC-1M-MB, BC-3M-MB, and BC-6M-MB).

In the first biomaterial (AAP), a medium broad peak was identified at approximately 3333.2 cm^{-1} related to the stretching of the O-H group, more precisely OH of polymeric molecules, due to being in the range 3200–3400 cm^{-1}; these molecules are possibly cellulose, the main component of wood. At approximately 1732.58 cm^{-1}, the stretching of the carbonyl group C=O was identified in a range characteristic of esters, which could be related to resins, grease, and waxes typical of *Aspidosperma polyneuron* wood. A sharp peak is observed at approximately 1030.84 cm^{-1}, corresponding to the C-OH bond of aromatic rings, probably related to the aromatic rings of lignin. Concerning CCS, a less pronounced peak is visualized at approximately 3255.81 cm^{-1}, which may be associated with the stretching of the OH group. In the CCS spectrum, the peaks observed in the

AAP spectrum from 1232 to 1732 cm^{-1} disappear, giving way to a single sharp rise at approximately 1581 cm^{-1} related to the functional group C=C, which indicates the release of volatile compounds in the carbonization process, obtaining a compact char. This shift of the representative peaks in the infrared spectrum between biomass and char was also observed between eucalyptus sawdust and biomaterial synthesized from it in the study by Chen et al. [42]. The peak at approximately 3000 and 3500 cm^{-1} corresponding to the stretching of the OH group is one of the peaks in which the release of volatiles during carbonization is most clear [42].

When comparing the spectra of the biomaterials functionalized with urea, it is observed in the BC-1M sample a peak at approximately 3245 cm^{-1} before the adsorption process, which can be attained to the stretching of the OH group. Moreover, a decrease in the vibration of this peak was observed for the other functionalized biocarbons (BC-3M and BC-6M), which can be related to increased urea concentration. This same behavior is observed with the peak, at BC-1M, at approximately 1223 cm^{-1}, related to the carboxyl group; this behavior may be described in the first case as the interaction between the OH group and the urea molecules, between which hydrogen bonds are formed according to what was reported by Sajjadi et al. [16]; in the second case, the interaction is between the OH group and the carboxyl group; decreasing the vibration of the OH group, this decrease is accentuated as the urea concentration increases. The FTIR analysis shows the comparison of the characteristic peaks of the main functional groups of the biomaterials before and after carbonization; the common peaks for all the biomaterials are those observed between 3000 and 3500 cm^{-1}, corresponding to the OH group, at approximately 1500 cm^{-1} corresponding to the stretching of the C=C bond of aromatic rings and at approximately 1200 cm^{-1} for the stretching of the C-O group, in addition, different peaks corresponding to the stretching of specific functional groups are observed.

3.5. Scanning Electron Microscopy

Figure 4a shows the SEM image of the sawdust of *Aspidosperma polyneuron* (AAP), showing a compact layered structure with few visible pores. In contrast, the unmodified CCS biomaterial shows a highly porous structure. This fact evidences the benefits of the biomass carbonization process, where volatile compounds are released from the sawdust and the carbon content is increased, as can be seen in Figure 4b.

In the SEM images of the biomaterials modified with urea (Figure 4c–e), it is evident that the effect of ultrasound substantially improved the presence of micropores, eliminating traces of ash and obtaining cleaner surfaces. From this, it can be ensured that the time in the ultrasound manages to open the pores clogged by-products of the carbonization process, increasing the porosity of the materials. For this reason, it can be ensured that it is not enough to carbonize the biomass without subsequent processes; in this case, ultrasonic washing, proposed by Sajjadi et al. [11], stands out, who compared commercial biochar, made from pine softwood without subsequent processes, with the same type of sonicated biochar and evaluated the difference of biochar's with SEM micrographs, finding results similar to those of the present study, because in the biochar's sonicated for 20, 40, and 60 s, open pores were observed. No lumps were visualized, while in the biochar without time in the ultrasound, they were observed the opposite.

Likewise, it is observed that the macropores are morphologically more defined in the CCS, while in the functionalized biomaterials, the deformation of the mesopores increases; this change in the morphology of the macropores is attributed to the activation with phosphoric acid. The amorphous surface structure of adsorbents favors the adsorption of contaminants since amorphous materials have the advantage of providing a higher surface area and higher number of active sites for adsorbate molecules compared to crystalline adsorbents, such As mentioned by Salehi et al. [18], who synthesized biochar's at different temperatures and observed a decrease in their crystallinity as the carbonization temperature increased, obtaining a higher percentage of adsorbate removal (MB in their case), with the amorphous biochar's synthesized at 400 °C and 500 °C.

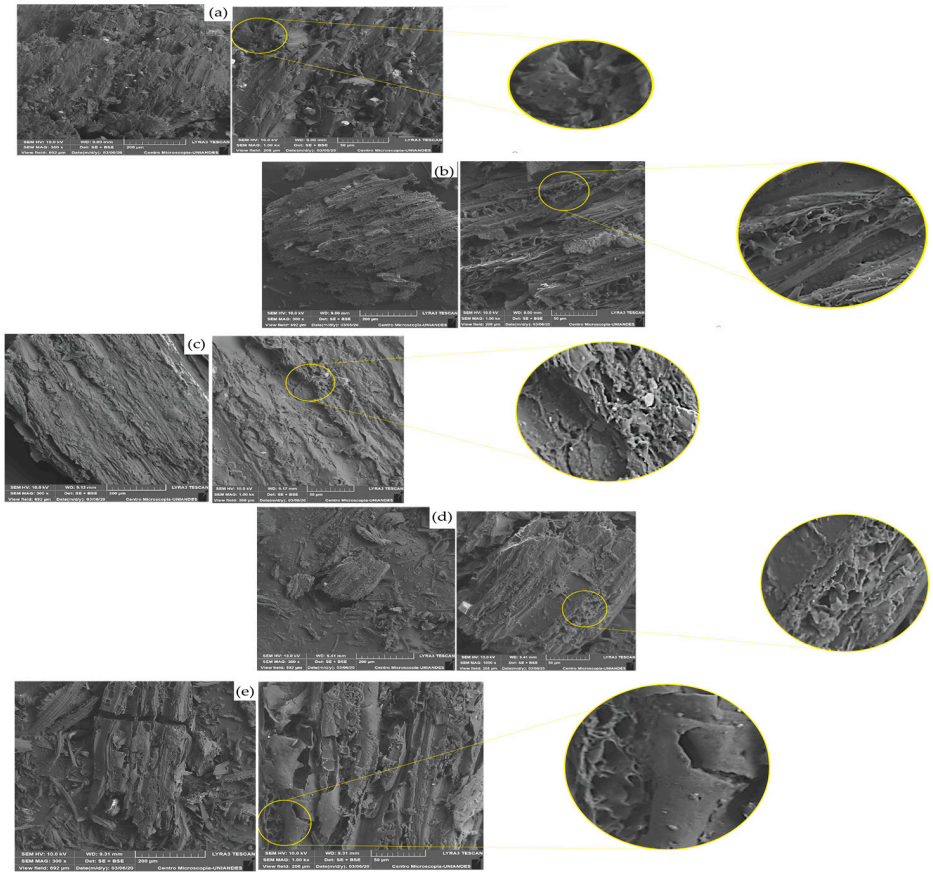

Figure 4. Scanning electron microscopy (SEM). (**a**) AAP, (**b**) CCS (**c**) BC-1M, (**d**) BC-3M, and (**e**) BC-6M.

3.6. Methylene Blue Adsorption Tests

The three levels of pH variation analyzed were 7, 8, and 9, which are above pH_{pzc}. The adsorbent dose was 0.035 g, and the contaminant concentration was 40 mg/L. Considering the replicates, the average adsorption capacity was calculated, and pH 7 was identified as the optimum pH because 75% of the evaluated biomaterials had the highest adsorption capacity at this pH. Figure 5 shows the effect of the solution's pH on methylene blue's adsorption capacity.

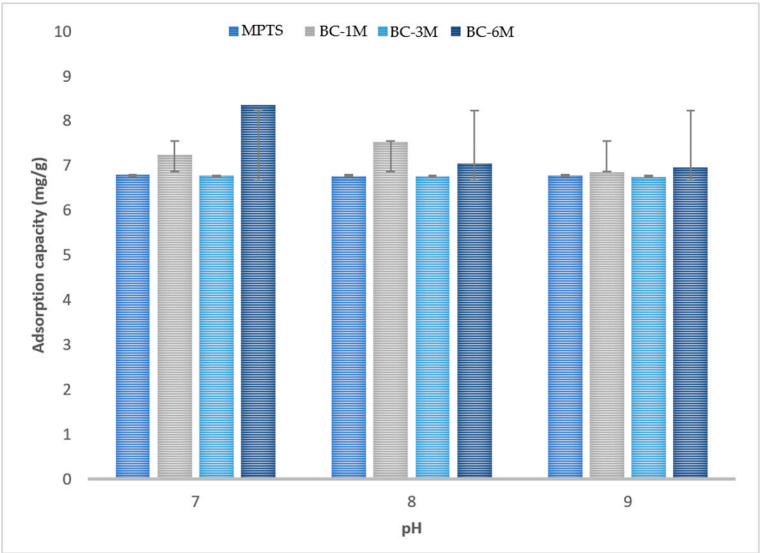

Figure 5. Effect of pH on the adsorption capacity of methylene blue average adsorption capacity to find the optimum pH.

One-factor ANOVA statistical was employed, establishing the null and alternative hypothesis to determine the effects of the initial pH of the contaminant solution on the methylene blue index:

H_0: The initial pH of the solution does not affect the methylene blue index.

H_a: The initial pH of the solution affects the methylene blue index.

A value of $p < 0.05$ was set as the criterion for statistical significance. Table 4 shows the ANOVA for methylene blue adsorption capacity. A value greater than 0.05 is observed in each case, which indicates that H_0 is not discarded, meaning that there are no significant differences between the means of the methylene blue index values when varying the initial pH concentration. Based on the above, it was decided to take pH 7 for the next adsorption test, which is the lowest pH level. It allowed obtaining the highest values of methylene blue index in three of the four adsorbents evaluated.

Table 4. ANOVA for methylene blue adsorption capacity.

Adsorbent	Source of Variation	Sum of Squares	Degrees of Freedom	F_0	*p* Value
CCS	Treatments	0.0014	2	3.92	0.1456
	Error	0.0005	3		
	Total	0.0019	5		
BC-1M	Treatments	0.4562	2	0.63	0.5915
	Error	1.0885	3		
	Total	1.5447	5		
BC-3M	Treatments	0.0009	2	1.47	0.3584
	Error	0.0009	3		
	Total	0.0018	5		
BC-6M	Treatments	2.4637	2	1.80	0.3063
	Error	2.0515	3		
	Total	4.5152	5		

Biomaterials are commonly produced from plant residues, including wood [31,42], tea [43], seaweed [44], corn stalk [45], lignin [46], water thistle husk [21], banana pseudo stem [47], soybean slag [48], bamboo, bagasse, and marabou cane [34]. These lignocellulosic materials are preferred for their abundance, particularly in the case of agroindustrial residues. They are transformed into biosorbents and other valuable products, such as fuels and fertilizers, to reduce waste emissions and carbon footprint, taking advantage of their economic potential [49]. Additionally, biomaterials are produced from other types of waste, such as activated sludge and municipal waste, including food, cardboard, paper, and yard waste [50–52]. Table 5 compares various studies documented in the scientific literature and the current research results on biochar synthesis.

Table 5. Comparison of chemically modified biomasses for methylene blue adsorption: preparation and characterization techniques.

Biomass	Synthesis Variables		Characterizations			References
			Methylene Blue (MB) Test		Techniques	
Sawdust mix	T (°C)	450	qe (mg/g)	32	SEM: Identification of the polymeric layer on the surface of the biochar. FTIR: Amide I and Amide II. Amino acids and proteins (1635 and 1565 cm^{-1}). Carboxylate ion (1395 cm^{-1}) and pectin pyranoid ring (1130 cm^{-1}). Phenolic O-H (1260 cm^{-1}) Organic phosphorus P–O and/or sugar C–O bond present in the biopolymer. pH_{pzx} = 7.95	[31]
	t (h)	4	Adsorbent dose (g/L)	1		
	Free of O_2	No				
	Modification	Biopolymer layer (Okra mucilage). Activation with NaOH	MB concentration (ppm)	25		
			pH	7		

Table 5. *Cont.*

Biomass	Synthesis Variables		Characterizations			References
			Methylene Blue (MB) Test		Techniques	
Eucalyptus wood	T (°C)	700	qe (mg/g)	112	SEM: Presence of channels in the form of columns and slits. FTIR: Peaks at 3000–3500 cm^{-1} for –OH groups; at 1799 cm^{-1} for C=O from carbonyl and carboxyl groups; 1579 cm^{-1} for C=C bonds; 1400 cm^{-1} for COO carboxylic groups; 1122 cm^{-1} for C-O bonds; 588, 622, 696, and 877cm^{-1} for FeO bonds. SBET = 645.23 m^2/g. Average pore diameter: 2.71 nm. Pore volume: 0.44 cm^3/g.	[42]
	t (h)	1 h, 15 min	Adsorbent dose (g/L)	1		
	Free of O_2	No				
	Modification	Activation with $FeCl_3$	MB concentration (ppm)	50		
			T (°C)	25		
Sawdust (PSAC) from the Pentace species	T (°C)	700	qe (mg/g)	42.58	SEM: Rough and uneven surface textures. Pores of different sizes and shapes were visualized. The chemical activation process produced pores on the carbon's surface and obtained carbon with a large surface area and a porous structure. FTIR: Peaks at 3611–3951 cm^{-1} for OH vibrations; 2720 cm^{-1} for C–H groups; 2335 cm^{-1} for C-C bonds; 1689 and 1520 cm^{-1} for C = O bonds and aromatic rings C = C, respectively; and 1269 cm^{-1} related to the C-O stretch of the phenolic group. SBET: 914.15 m^2/g, Pore volume: 0.52 cm^3/g. Average pore diameter: 3.19 nm.	[53]
	t (h)	2	Adsorbent dose (g/L)	1		
	Free of O_2	Yes				
	Modification	Activation with KOH	MB concentration (ppm)	50		
			pH	7		
Sawdust	T (°C)	425	qe (mg/g)	210	SEM: The surface textures of the precursors were rough and uneven. Pores of different sizes and shapes were evident. FTIR: Peaks at 3420 cm^{-1} for OH groups; 2926 and 2853 cm^{-1} for CH groups; 1458 and 1377 cm^{-1} for C=O bonds; 1704 cm^{-1} for COO^- groups; and P-containing groups at 1167 cm^{-1} for C-O-P formed by the reaction of phosphorus oxides. SBET: 1504 m^2/g. Pore volume: 0.78 cm^3/g.	[54]
	t (h)	2	Adsorbent dose (g/L)	-		
	Free of O_2	Yes				
	Modification	Activation with H_3PO_4 assisted with ultrasound for 5 min	MB concentration (ppm)	-		
			pH	-		
Sugarcane bagasse	T (°C)	400	qe (mg/g)	15	Pycnometric density: 1.09 g/mL. Bulk density: 0.28 g/mL. Total porosity: 74%. Fixed Coal: 12%. Bulk density: 0.33 g/mL. Average pore radius: 535 nm.	[34]
	t (h)	1	Adsorbent dose (g/L)	-		
	Free of O_2	No				
	Modification	Activation first with H_3PO_4 followed of activation with HNO_3	MB concentration (ppm)	-		
			pH	-		
Sugarcane bagasse	T (°C)	600	qe (mg/g)	15	Pycnometric density: 1.09 g/mL. Bulk density: 0.28 g/mL. Total porosity: 74%. Fixed Coal: 12%. Apparent density: 0.28 g/mL. SBET: 305 m^2/g. pH_{pzx}: 6.1.	[40]
	t (h)	2	Adsorbent dose (g/L)	-		
	Free of O_2	No				
	Modification	Activation first with H_3PO_4 followed of activation with HNO_3	MB concentration (ppm)	-		
			pH	-		
Tea residue	T (°C)	700	qe (mg/g)	48.39	SEM: Porous channel structure rich and well developed, better than unmodified biochar. Elemental analysis by EDS: Detection of C, N, O, Na, and K atoms with a concentration of 81.29%, 8.79%, 6.19%, 1.59%, and 0.03%, respectively. SBET: 178 m^2/g, Pore volume: 0.164 cm^3/g.	[43]
	t (h)	4	Adsorbent dose (g/L)	1		
	Free of O_2	No				
	Modification	Activation with NaOH at 10% *w*/*w*	MB concentration (ppm)	50		
			pH	10		
Tea residue	T (°C)	300	qe (mg/g)	31.46	SEM: Semi-finished porous structure was observed. FTIR: Peaks at 3413 cm^{-1} for OH groups; 2921 cm^{-1} and 2851 cm^{-1} for -CH bonds; 1613 cm^{-1} for secondary amine; 1440 cm^{-1} for C-C bonds in aromatic rings; 1000–1163 cm^{-1} for C-O groups; and bands at 960–970 cm^{-1} for C–H bonds in aromatic rings. SBET: 1.9 m^2/g. Pore volume: 0.0048 cm^3/g.	[30]
	t (h)	-	Adsorbent dose (g/L)	1.3		
	Free of O_2	Yes				
	Modification	Activation with H_3PO_4	MB concentration (ppm)	50		
			pH	9.65		
Lignin	T (°C)	400	qe (mg/g)	162.93	SEM: Biochar samples have micropore structure. Unmodified and modified biochar samples had similar pore diameter distributions. FTIR: Peaks at 3442 cm^{-1} for OH groups; 1620 cm^{-1} for C-H groups in aromatic ring; 1384 cm^{-1} for -CH_2 and -CH_3 groups; 1262 cm^{-1} for ether bond; and 1082 cm^{-1} for C-O bond. SBET: 349.646 m^2/g. Average pore diameter: 2.184 nm. Pore width: 1.178 nm. Pore volume: 0.029 cm^3/g.	[46]
	t (h)	1	Adsorbent dose (g/L)	-		
	Free of O_2	No				
	Modification	Modification with MnO_2	MB concentration (ppm)	50		
			pH	12		

Table 5. *Cont.*

Biomass	Synthesis Variables		Characterizations			References
			Methylene Blue (MB) Test		Techniques	
Banana pseudostem	T (°C)	200	qe (mg/g)	81.54	SEM: It has a mesopore structure. The modified biochar showed smaller pore size, which could be caused by Mo filling in the pores or pore collapse. FTIR: Peaks at 3440 cm^{-1} for OH groups; 2927 cm^{-1} for C-H groups; 1595 and 1642 cm^{-1} attributed to C-O and C-C groups, respectively; 1434 and 1449 cm^{-1} for C-C groups in aromatics; 1040 and 1097 cm^{-1} for C-O bonds in aliphatic and aromatic structures; 951 and 799 cm^{-1} for Mo-O bonds. Average pore diameter: 43.283 µm. Pore diameter: 14.33 nm, Pore volume: 0.01234 cm^3/g. SBET: 3.741 m^2/g.	[47]
	t (h)	1	Adsorbent dose (g/L)	0.5		
	Free of O_2	Yes				
	Modification	Phosphomolybdic acid	MB concentration (ppm)	50		
			pH	7		
Seaweed (*Gelidiella acerosa*)	T (°C)	800	qe (mg/g)	96	SEM/EDS: Pores and cavities are observed on the surface/C (72.96%), O (15.03%), N (5.78%) and S (6.22%). FTIR: Peaks at 3440 cm^{-1} for O–H group; 1625 cm^{-1} for primary amine N–H group; 1389 cm^{-1} for N–O group; 1168 and 1127 cm^{-1} for C–O group. SBET: 926.39 m^2/g. Mesopore volume and size: 0.57 cm^3/g and 2.45 nm, respectively.	[44]
	t (h)	3	Adsorbent dose (g/L)	1		
	Free of O_2	Yes				
	Modification	The biomass was washed with HCl and distilled water at pH 6.5	MB concentration (ppm)	100		
			pH	7		
Fir sawdust	T (°C)	400	qe (mg/g)	0.38	SEM: Irregular sheet-like structure, sparse texture, and presence of few small pores on the carbon surface. FTIR: Peaks at 3700 cm^{-1} for O-H group; 2840 and 2349 cm^{-1} for C–H and O=C=O groups, respectively; 1650 cm^{-1} for C–H bond; 1050 cm^{-1} for C-O group; and 875 for C-Cl bond. Elemental analysis by EDS: Detection of C, Ca, Si, Al, K, and S atoms with a concentration of 78.03%, 18.64%, 1.469%, 0.562%, 0.103%, and 0.139%, respectively.	[55]
	t (h)	-	Adsorbent dose (g/L)	30		
	Free of O_2	Yes				
	Modification	No	MB concentration (ppm)	60		
			pH	6.5		
Water caltrop shell	T (°C)	750	qe (mg/g)	125	SEM: Small pores were observed in addition to a rigid frame on the surface of the resulting carbon. SBET: 810.5 ± 25.7 m^2/g. Pore volume: 0.441 ± 0.024 cm^3/g. Average pore diameter: 21.7 ± 0.8 Å. Real density: 1.787 g/cm^3. Particle density: 0.999 g/cm^3. Porosity: 0.441.	[21]
	t (h)	1.5	Adsorbent dose (g/L)	0.15		
	Free of O_2	Yes				
	Modification	No	MB concentration (ppm)	20		
			pH	7		
Soybean dross	T (°C)	800	qe (mg/g)	996.37	FTIR: Peaks at 3411 cm^{-1} for O-H group; 2933 cm^{-1} for C-H bond; 1710 and 1587 cm^{-1} for C = O and C = C bonds; 1095 cm^{-1} for C-OH bond. SEM: Random pore structures were evident on the surface after high-temperature activation with $KHCO_3$. SBET: 1620 m^2/g. Elemental analysis by EDS: Detection of C, O, H, N, and S atoms with a concentration of 66.28%, 28.11%, 1.67%, 0.542%, and 0.383%, respectively. Pore volume: 0.7509 cm^3/g. Average pore diameter: 1.859 nm. Yield: 15.61%.	[48]
	t (h)	-	Adsorbent dose (g/L)	1		
	Free of O_2	Yes				
	Modification	Activated with $KHCO_3$	MB concentration (ppm)	1000		
			pH			
Corn stalk	T (°C)	300	qe (mg/g)	16.41	SEM: Increased pores were observed on the surface after biomass modification. FTIR: Peaks at 3410 cm^{-1} for O–H group; 2925 and 2842 cm^{-1} for -CH_3 and -CH_2 groups; 1680 and 1430 cm^{-1} for vibration of the benzene ring; 1109 cm^{-1} for C-O bond from phenols and oxyhydrogen groups; 873 cm^{-1} due to weaker aromatization. SBET: 2.56 m^2/g. Pore volume: 0.00864 cm^3/g Average pore diameter: 13.5 nm.	[45]
	t (h)	1	Adsorbent dose (g/L)	2		
	Free of O_2	Yes				
	Modification	Modification with $MgCl_2$	MB concentration (ppm)	45		
			pH			
Mixture of food, garden, paper, and cardboard waste	T (°C)	300	qe (mg/g)	5.018	SEM: It was evaluated two samples of BC from paper/cardboard and food/garden, showing differences in the structure of the surface, demonstrating the variability of the structure of carbons from this type of waste. FTIR: Peaks at 1416, 873, and 712 cm^{-1} for CO_3 presence; peaks between 3500 and 3000 cm^{-1} for OH groups; and peaks between 1550 and 1350 cm^{-1} for calcite.	[56]
	t (h)	12	Adsorbent dose (g/L)	5		
	Free of O_2	Yes				
	Modification	No	MB concentration (ppm)	75		
			pH	5		
Sewage sludge	T (°C)	180 °C in drying oven	qe (mg/g)	15.77	FTIR: Peaks at 3420 cm^{-1} for OH group; 2920 and 2853 cm^{-1} for methylene; 1630 and 1030 cm^{-1} for carbonyl; and 575 cm^{-1} attributed to Fe-O.	[57]
	t (h)	12 h	Adsorbent dose (g/L)	0.5		
	Free of O_2	No (hydro thermal process)				
	Modification	Mixing and carbonization with Fe-rich sludge (by-product of groundwater purification).	MB concentration (ppm)	10		
			pH			

Table 5. *Cont.*

Biomass	Synthesis Variables		Characterizations			References
			Methylene Blue (MB) Test		Techniques	
Sawdust from *Aspidosperma polyneuron*	T (°C)	250	qe (mg/g)	12.45	FTIR: Peak at 3183 cm^{-1} for OH group; 1586 cm^{-1} for C = C bond from the aromatic ring; 1215 cm^{-1} for carboxyl group; peaks from 581 to 533 cm^{-1} for hydrocarbon groups of single, double, and triple bonds. SEM/EDS: Porous surface was observed; however, the pores decreased in size with respect to the urea concentration. Elemental analysis by EDS: Detection of C and O atoms with a concentration of 68.45% and 31.55%, respectively. Actual density: 0.783 g/cm^3. Porosity: 0.604. pHpzc: 5.6	Present study
	t (h)	0.5	Adsorbent dose (g/L)	3.5		
	Free of O_2	No				
	Modification	Activation with H_3PO_4 and functionalization with urea (6M)	MB concentration (ppm)	60		
			pH	7		

After studying the synthesis of biomaterials at temperatures between 180 and 400 °C, it was observed that the BC-6M sample exhibited a lower methylene blue adsorption capacity than 75% of the analyzed studies. However, it was found that the BC-6M sample has a similar adsorption capacity compared to at least four other studies with q_e values higher than the BC-6M sample. On the other hand, waste mixtures [56] and spruce sawdust [55] biomaterials showed even lower methylene blue adsorption capacity than the BC-6M sample. However, in the case of waste mixtures, it was observed that the carbonization temperature was 50 °C higher than that of the BC-6M sample, with a longer residence time and an inert atmosphere. In the case of spruce sawdust biomaterial, it was observed that the carbonization temperature was 150 °C higher than the BC-6M sample, with a higher adsorbent dosage and an inert atmosphere. All these variables contribute to an increase in the porosity of the biomaterials and, therefore, their methylene blue adsorption capacity. However, due to the good physicochemical characteristics of the BC-6M sample, such as sonication processes, activation with phosphoric acid, and functionalization with 6M urea, it has a better q_e value. In conclusion, the BC-6M biomaterial can be a practical option for removing textile dye.

4. Conclusions

This study investigated the effectiveness of AAP-derived biomaterials for their ability to remove textile dyes. The biomaterials were modified with phosphoric acid and functionalized with urea at different concentrations; furthermore, their adsorption capacity was evaluated using the methylene blue method. The best results were achieved at a synthesis process temperature of 250 °C for 30 min. The physical characterization of sawdust before biomaterial synthesis showed that over 48% of the AAP biomaterial fraction had a size of less than 0.428 mm, which was beneficial for adsorption since the synthesized biomaterials had small particle sizes and high surface area.

The BC-6M biomaterial stood out with a methylene blue adsorption index of 12.4 mg/g due to its favorable physicochemical properties derived from sonication, activation with phosphoric acid, and functionalization with 6M urea. SEM analysis revealed significant improvements in the morphology of the urea-modified biomaterials, mainly due to the application of ultrasound, which opened clogged pores and increased the porosity of the materials. Phosphoric acid activation also affected macropore morphology, while the amorphous surface structure of the adsorbents improved adsorption capacity by providing a greater surface area and more active sites for adsorbate molecules.

These findings suggest that functionalized biomaterials are effective for contaminant removal, with the BC-6M biomaterial showing promise as a candidate. Combining techniques such as sonication and chemical activation can potentially improve the properties of biomaterials for adsorption applications. These results contribute to a better understanding of the relationship between material morphology and performance in removing contaminants and offer new perspectives for designing and developing effective and sustainable biomaterials.

Author Contributions: Conceptualization, Á.V.-O., C.T.-T. and A.H.-B. Data curation, R.O.-T., C.T.-T. and A.H.-B. Formal analysis, Á.V.-O., A.H.-B. and D.C.-S. Funding acquisition, C.T.-T. Investigation, D.C.-S. Methodology, Á.V.-O., C.T.-T. and D.C.-S. Project administration, Á.V.-O. and C.T.-T. Resources, C.T.-T. Software, C.T.-T. Supervision, Á.V.-O. and A.H.-B. Validation, C.T.-T. and R.O.-T. Visualization, R.O.-T. and A.H.-B. Writing—original draft, D.C.-S. Writing—review and editing, R.O.-T. and A.H.-B. All authors have read and agreed to the published version of the manuscript.

Funding: This research received no external funding.

Data Availability Statement: The data that support the results of this study are available on request from the corresponding author.

Acknowledgments: The authors thank the University of Cartagena for providing the materials and equipment required for this study.

Conflicts of Interest: The authors declare no conflict of interest.

Appendix A

Table A1. Detailed calculation of the apparent density for the biomaterials.

Sample	Weight (g)	Volume (cm^3)	Apparent Density (g/cm^3)
AAP	1.080	3	0.360
CCS	0.840	3	0.280
BC-1M	0.930	3	0.310
BC-3M	0.908	3	0.303
BC-6M	0.930	3	0.310

Table A2. Detailed calculation of the porosity for the biomaterials.

Sample	Sample Weight (g)	Sample Weight + Water (g)	Real Density (g/cm^3)	Porosity %
AAP	1.26	10.87	2.455	85.3
CCS	0.55	8.8	0.296	0.5
BC-1M	0.49	9.1	0.327	5.1
BC-3M	0.38	9.26	0.308	1.8
BC-6M	0.75	9.91	0.783	60.4

Table A3. Calculation of surface-volume diameter, mass-mean diameter, and arithmetic mean diameter.

Passing Fraction	Particle Number	$\Delta Ø/D_{pi}$	N_i*D_{pi}	$\Delta Ø*D_{pi}$
1	-	-	-	-
0.939	0.002	0.041	0.004	0.091
0.618	0.101	0.428	0.075	0.241
0.482	0.229	0.317	0.098	0.058
0.282	1.158	0.705	0.328	0.057
0.174	2.409	0.598	0.436	0.020
0.080	5.952	0.739	0.762	0.012
	N_T	$\sum \Delta Ø/Dpi$	$\sum Ni*Dpi$	$\sum \Delta Ø*Dpi$
	9.851	2.827	1.703	0.479
		Shape factor (a)		0.524
		Particle density (Kg/cm^3)		2455
		S-V diameter (mm)		0.354
		Arithmetic mean diameter (mm)		0.173
		Mass median diameter (mm)		0.479

References

1. Sahina, S.C.; Aksub, S. Adsorption of dyes from aqueous textile byproducts on activated carbon from scenedesmus obliquus. *Anal. Lett.* **2017**, *50*, 1812–1830. [CrossRef]
2. Zhang, L.; Lei, M.; Feng, T.; Chang, W.; Ye, A.; Yi, H.; Yi, C. A case study of the wastewater treatment system modification in denim textile industry. *J. Text. Inst.* **2021**, *112*, 1666–1670. [CrossRef]
3. Vyavahare, G.D.; Gurav, R.G.; Jadhav, P.P.; Patil, R.R.; Aware, C.B.; Jadhav, J.P. Response surface methodology optimization for sorption of malachite green dye on sugarcane bagasse biochar and evaluating the residual dye for phyto and cytogenotoxicity. *Chemosphere* **2018**, *194*, 306–315. [CrossRef] [PubMed]
4. Chung, K.T. Azo dyes and human health: A review. *J. Environ. Sci. Health Part C* **2016**, *34*, 233–261. [CrossRef]
5. Shaheen, S.M.; Niazi, N.K.; Hassan, N.E.E.; Bibi, I.; Wang, H.; Tsang, D.C.W.; Ok, Y.S.; Bolan, N.; Rinklebe, J. Wood-based biochar for the removal of potentially toxic elements in water and wastewater: A critical review. *Int. Mater. Rev.* **2019**, *64*, 216–247. [CrossRef]
6. Kuang, Y.; Zhang, X.; Zhou, S. Adsorption of Methylene Blue in Water onto Activated Carbon by Surfactant Modification. *Water* **2020**, *12*, 587. [CrossRef]
7. Zbair, M.; Anfar, Z.; Khallok, H.; Ahsaine, H.A.; Ezahri, M.; Elalem, N. Adsorption kinetics and surface modeling of aqueous methylene blue onto activated carbonaceous wood sawdust. *Fuller. Nanotub. Carbon Nanostructures* **2018**, *26*, 433–442. [CrossRef]
8. Bernal, L.A.; Hernández, M.K.; Berber, M.S.; Martínez, M.E.; Delgado, R.D.; Espinosa, M.Á. Removal of compound dye remazol orange from wastewater generated in the textile industry. *Av. Cienc. Ing.* **2017**, *8*, 51–57.
9. Ardila-Ramírez, C.; Palacio-Londoño, Á.; Barrera-Zapata, R. Pinneapple peel as adsorbent of typical textile industry dyes. *Cienc. Desarro.* **2018**, *9*, 161–168.
10. Li, L.; Yang, M.; Lu, Q.; Zhu, W.; Ma, H.; Dai, L. Oxygen-rich biochar from torrefaction: A versatile adsorbent for water pollution control. *Bioresour. Technol.* **2019**, *294*, 122142. [CrossRef]
11. Alshammari, M.; Essawy, A.A.; El-Nggar, A.M.; Sayyah, S.M. Ultrasonic-Assisted Synthesis and Characterization of Chitosan-Graft-Substituted Polyanilines: Promise Bio-Based Nanoparticles for Dye Removal and Bacterial Disinfection. *J. Chem.* **2020**, *2020*, 3297184. [CrossRef]
12. Bortoluz, J.; Ferrarini, F.; Bonetto, L.R.; da Silva Crespo, J.; Giovanela, M. Use of low-cost natural waste from the furniture industry for the removal of methylene blue by adsorption: Isotherms, kinetics and thermodynamics. *Cellulose* **2020**, *27*, 6445–6466. [CrossRef]
13. Bhowmik, S.; Chakraborty, V.; Das, P. Batch adsorption of indigo carmine on activated carbon prepared from sawdust: A comparative study and optimization of operating conditions using Response Surface Methodology. *Results Surf. Interfaces* **2021**, *3*, 100011. [CrossRef]
14. Sun, L.; Chen, D.; Wan, S.; Yu, Z. Performance, kinetics, and equilibrium of methylene blue adsorption on biochar derived from eucalyptus saw dust modified with citric, tartaric, and acetic acids. *Bioresour. Technol.* **2015**, *198*, 300–308. [CrossRef] [PubMed]
15. Oyewo, O.A.; Adeniyi, A.; Sithole, B.B.; Onyango, M.S. Sawdust-Based Cellulose Nanocrystals Incorporated with ZnO Nanoparticles as Efficient Adsorption Media in the Removal of Methylene Blue Dye. *ACS Omega* **2020**, *5*, 18798–18807. [CrossRef]
16. Sajjadi, B.; Broome, J.W.; Chen, W.Y.; Mattern, D.L.; Egiebor, N.O.; Hammer, N.; Smith, C.L. Urea functionalization of ultrasound-treated biochar: A feasible strategy for enhancing heavy metal adsorption capacity. *Ultrason. Sonochem.* **2019**, *51*, 20–30. [CrossRef]
17. Kasera, N.; Hall, S.; Kolar, P. Effect of surface modification by nitrogen-containing chemicals on morphology and surface characteristics of N-doped pine bark biochars. *J. Environ. Chem. Eng.* **2021**, *9*, 105161. [CrossRef]
18. Kalak, T.; Kaczmarek, M.; Nowicki, P.; Pietrzak, R.; Tachibana, Y.; Cierpiszewski, R. Preparation of nitrogen-enriched pine sawdust-based activated carbons and their application for copper removal from the aquatic environment. *Wood Sci. Technol.* **2022**, *56*, 1721–1742. [CrossRef]
19. Chen, X.; Li, H.; Liu, W.; Meng, Z.; Wu, Z.; Wang, G.; Liang, Y.; Bi, S. Low-temperature constructing N-doped graphite-like mesoporous structure biochar from furfural residue with urea for removal of chlortetracycline from wastewater and hydrothermal catalytic degradation mechanism. *Colloids Surfaces A Physicochem. Eng. Asp.* **2020**, *600*, 124873. [CrossRef]
20. *ASTM C136/C136M-19*; Standard Test Method for Sieve Analysis of Fine and Coarse Aggregates. ASTM: West Conshohocken, PA, USA, 2020.
21. Lin, Y.Q.; Tsai, W.T. Liquid-Phase Removal of Methylene Blue as Organic Pollutant by Mesoporous Activated Carbon Prepared from Water Caltrop Husk Using Carbon Dioxide Activation. *Processes* **2021**, *9*, 238. [CrossRef]
22. Ovhal, S.D.; Rodrigues, C.S.D.; Madeira, L.M. Photocatalytic wet peroxide assisted degradation of Orange II dye by reduced graphene oxide and zeolites. *J. Chem. Technol. Biotechnol.* **2021**, *96*, 349–359. [CrossRef]
23. *ASTM D 3860-98*; Standard Practice for Determination of Adsorptive Capacity of Activated Carbon by Aqueous Phase Isotherm Technique. ASTM: West Conshohocken, PA, USA, 2014.
24. Ramakrishnan, R.K.; Padil, V.V.T.; Wacławek, S.; Černík, M.; Varma, R.S. Eco-Friendly and Economic, Adsorptive Removal of Cationic and Anionic Dyes by Bio-Based Karaya Gum—Chitosan Sponge. *Polymers* **2021**, *13*, 251. [CrossRef] [PubMed]
25. Hou, Y.; Yan, S.; Huang, G.; Yang, Q.; Huang, S.; Cai, J. Fabrication of N-doped carbons from waste bamboo shoot shell with high removal efficiency of organic dyes from water. *Bioresour. Technol.* **2020**, *303*, 122939. [CrossRef]

26. Paolella, M.S. *Linear Models and Time-Series Analysis: Regression, ANOVA, ARMA and GARCH*; John Wiley & Sons: Hoboken, NJ, USA, 2018.
27. Tejada-Tovar, C.; Villabona-Ortíz, A.; Ortega-Toro, R. Determination of Kinetic Parameters in the Biosorption of Chromium (VI) in Aqueous Solution. *Ing. Cienc.* **2020**, *16*, 129–143. [CrossRef]
28. Krysanova, K.; Krylova, A.; Kulikova, M.; Kulikov, A.; Rusakova, O. Biochar characteristics produced via hydrothermal carbonization and torrefaction of peat and sawdust. *Fuel* **2022**, *328*, 125220. [CrossRef]
29. Qin, F.; Zhang, C.; Zeng, G.; Huang, D.; Tan, X.; Duan, A. Lignocellulosic biomass carbonization for biochar production and characterization of biochar reactivity. *Renew. Sustain. Energy Rev.* **2022**, *157*, 112056. [CrossRef]
30. Salehi, E.; Askari, M.; Velashjerdi, M.; Arab, B. Phosphoric acid-treated Spent Tea Residue Biochar for Wastewater Decoloring: Batch Adsorption Study and Process Intensification using Multivariate Data-based Optimization. *Chem. Eng. Process.-Process Intensif.* **2020**, *158*, 108170. [CrossRef]
31. Nath, H.; Saikia, A.; Goutam, P.J.; Saikia, B.K.; Saikia, N. Removal of methylene blue from water using okra (*Abelmoschus esculentus* L.) mucilage modified biochar. *Bioresour. Technol. Reports* **2021**, *14*, 100689. [CrossRef]
32. Prías, J.J.; Rojas, C.A.; Echeverry, N.A.; Fonthal, G.; Ariza, H. Identification of optimal variables from the precursor Guadua angustifolia Kunth. *Rev. Acad. Colomb. Cienc. Exactas Físicas Nat.* **2011**, *35*, 157–166.
33. Saletnik, B.; Saletnik, A.; Zaguła, G.; Bajcar, M.; Puchalski, C. The Use of Wood Pellets in the Production of High Quality Biocarbon Materials. *Materials* **2022**, *15*, 4404. [CrossRef]
34. Prieto García, J.O.; Pérez Leiva, A.; Curbelo Sánchez, A.E.; Enríquez García, M.; Mollineda Trujillo, Á. Adsorption of lead (II) ions in isothermal conditions using activated carbon from sugarcane bagasse, marabou and bamboo. *Cent. Azúcar* **2021**, *48*, 21–28.
35. Velázquez-Maldonado, J.; Juárez-López, P.; Anzaldo-Hernández, J.; Alejo-Santiago, G.; Valdez-Aguilar, L.A.; Alia-Tejacal, I.; López-Martínez, V.; Guillén-Sánchez, G.A.; Dagoberto, P.-A. Nutrient concentration of rice husk biochar. *Rev. Fitotécnica Mex.* **2019**, *42*, 129–136.
36. Yang, C.D.; Lu, S.G. Effects of five different biochars on aggregation, water retention and mechanical properties of paddy soil: A field experiment of three-season crops. *Soil Tillage Res.* **2021**, *205*, 104798. [CrossRef]
37. Anggraeni, S.; Chelvina, G.; Girsang, S.; Bayu, A.; Nandiyanto, D.; Roild Bilad, M. Effects of particle size and composition of sawdust/carbon from rice husk on the briquette performance. *J. Eng. Sci. Technol.* **2021**, *16*, 2298–2311.
38. Serret-Guasch, N.; Giralt-Ortega, G.; Quintero-Ríos, M. Characterization of Sawdust of different Woods. *Tecnol. Química* **2016**, *36*, 395–405.
39. Mengist, M.; Woldeyes, B.; Gabbiye, N. Production and Characterization of Sawdust Briquettes for Firewood Substitution. In *International Conference on Advances of Science and Technology*; Springer: Cham, Switzerland, 2021; Volume 384, pp. 3–26.
40. Prieto García, J.O.; Gehan Geulamussein, N.; Pérez Leiva, A.; Martínez Albelo, E.; Enríquez García, M. Adsorption of Cadmium from an Aqueous Solution on Activated Coal from Bagasse of Sugarcane Roxa Variety. *Rev. Cent. Azúcar* **2020**, *47*, 1. Available online: http://centroazucar.uclv.edu.cu/index.php/centro_azucar/article/view/172 (accessed on 27 August 2023).
41. Daza Barranco, L.M.; Orrego, M.J.F.; Fernández Hincapie, J.J. Preparation and characterization of activated carbons from coal of Cesar's basin (Colombia). *Rev. Politécnica* **2018**, *14*, 75–88. [CrossRef]
42. Chen, Y.D.; Lin, Y.C.; Ho, S.H.; Zhou, Y.; Ren, N.Q. Highly efficient adsorption of dyes by biochar derived from pigments-extracted macroalgae pyrolyzed at different temperature. *Bioresour. Technol.* **2018**, *259*, 104–110. [CrossRef]
43. Mu, Y.; Ma, H. NaOH-modified mesoporous biochar derived from tea residue for methylene Blue and Orange II removal. *Chem. Eng. Res. Des.* **2021**, *167*, 129–140. [CrossRef]
44. Ahmed, M.J.; Okoye, P.U.; Hummadi, E.H.; Hameed, B.H. High-performance porous biochar from the pyrolysis of natural and renewable seaweed (*Gelidiella acerosa*) and its application for the adsorption of methylene blue. *Bioresour. Technol.* **2019**, *278*, 159–164. [CrossRef]
45. Zuo, H.; Qin, X.; Liu, Z.; Fu, Y. Preparation and characterization of modified corn stalk biochar. *BioResources* **2021**, *16*, 7428–7443. [CrossRef]
46. Liu, X.J.; Li, M.F.; Singh, S.K. Manganese-modified lignin biochar as adsorbent for removal of methylene blue. *J. Mater. Res. Technol.* **2021**, *12*, 1434–1445. [CrossRef]
47. Liu, S.; Li, J.; Xu, S.; Wang, M.; Zhang, Y.; Xue, X. A modified method for enhancing adsorption capability of banana pseudostem biochar towards methylene blue at low temperature. *Bioresour. Technol.* **2019**, *282*, 48–55. [CrossRef] [PubMed]
48. Ying, Z.; Chen, X.; Li, H.; Liu, X.; Zhang, C.; Zhang, J.; Yi, G. Efficient Adsorption of Methylene Blue by Porous Biochar Derived from Soybean Dreg Using a One-Pot Synthesis Method. *Molecules* **2021**, *26*, 661. [CrossRef] [PubMed]
49. Llenque-Díaz, L.A.; Quintana, A.; Torres, L.; Segura, R. Bioethanol production from organic plant waste. *Rebiol* **2020**, *40*, 21–29. [CrossRef]
50. Jayakrishnan, U.; Deka, D.; Das, G. Waste as feedstock for polyhydroxyalkanoate production from activated sludge: Implications of aerobic dynamic feeding and acidogenic fermentation. *J. Environ. Chem. Eng.* **2021**, *9*, 105550. [CrossRef]
51. Haile, A.; Gelebo, G.G.; Tesfaye, T.; Mengie, W.; Mebrate, M.A.; Abuhay, A.; Limeneh, D.Y. Pulp and paper mill wastes: Utilizations and prospects for high value-added biomaterials. *Bioresour. Bioprocess.* **2021**, *8*, 35. [CrossRef]
52. Le Pera, A.; Sellaro, M.; Bencivenni, E.; D'Amico, F. Environmental sustainability of an integrate anaerobic digestion-composting treatment of food waste: Analysis of an Italian plant in the circular bioeconomy strategy. *Waste Manag.* **2022**, *139*, 341–351. [CrossRef]

53. Khasri, A.; Bello, O.S.; Ahmad, M.A. Mesoporous activated carbon from Pentace species sawdust via microwave-induced KOH activation: Optimization and methylene blue adsorption. *Res. Chem. Intermed.* **2018**, *44*, 5737–5757. [CrossRef]
54. Zhang, Z.B.; Liu, X.Y.; Li, D.W.; Gao, T.T.; Lei, Y.Q.; Wu, B.G.; Zhao, J.W.; Wang, Y.K.; Wei, L. Effects of the ultrasound-assisted H3PO4 impregnation of sawdust on the properties of activated carbons produced from it. *New Carbon Mater.* **2018**, *33*, 409–416. [CrossRef]
55. Jock, A.A.; Joel, A.S.; Olubajo, O.O.; Zang, C.U.; Ayuba, M.S.; Wakili, P.T. Development of activated carbon from sawdust by pyrolysis and methylene blue adsorption. *Int. J. Chem. React. Eng.* **2021**, *19*, 473–481. [CrossRef]
56. Hoslett, J.; Ghazal, H.; Mohamad, N.; Jouhara, H. Removal of methylene blue from aqueous solutions by biochar prepared from the pyrolysis of mixed municipal discarded material. *Sci. Total Environ.* **2020**, *714*, 136832. [CrossRef] [PubMed]
57. Zeng, H.; Qi, W.; Zhai, L.; Wang, F.; Zhang, J.; Li, D. Magnetic biochar synthesized with waterworks sludge and sewage sludge and its potential for methylene blue removal. *J. Environ. Chem. Eng.* **2021**, *9*, 105951. [CrossRef]